Journal of JSCE, Vol. 2, 323-330, 2014
(Originally published in Journal of Japan Society of Civil Engineers, Ser. E1, Vol. 69, No. 3, I_17-I_24, 2013 in Japanese)

AUTOMATIC DETECTION OF SURFACE DISTRESS DUE TO FROST HEAVING ON EXPRESSWAYS BY USE OF AN ACCELEROMETER-BASED PROFILOMETER

Kazuya TOMIYAMA[1], Akira KAWAMURA[2] and Tomonori OHIRO[3]

[1]Member of JSCE, Assistant Professor, Dept. of Civil and Environmental Eng., Kitami Institute of Technology
(165 Koen-cho, Kitami, 090-8507, Japan)
E-mail : tomiyama@mail.kitami-it.ac.jp
[2] Member of JSCE, Professor, Dept. of Civil and Environmental Eng., Kitami Institute of Technology
(165 Koen-cho, Kitami, 090-8507, Japan)
[3]Research Engineer, Nexco-Engineering Hokkaido Co. Ltd.
(3-20 4-chome, Higashi Sapporo 5-jo, Shiroishi-ku, Sapporo, 003-0005, Japan)

In today's socio-economic situations, as pavement infrastructures have aged, road agencies are obliged to monitor their pavements frequently and effectively. This study examines an automatic detection method of surface distress due to frost heaving on expressways. The result shows that an accelerometer-based profilometer can accurately detect the distress in the roughness profile by the lifting wavelet filters developed on the basis of lifting scheme theory. The filters especially respond to the severe distress similar to the distress learned for the lifting scheme that needs careful monitoring. Therefore, we conclude that the automatic distress detection method based on the lifting scheme theory improves the ability of acceleration-based profilometer that contribute to daily monitoring activities by road agencies.

Key Words*: surface distress, frost heaving, accelerometer, lifting scheme, wavelet, pavement monitoring*

1. INTRODUCTION

Expressway pavements require the improvement of surface smoothness according to users' demand to keep both driving and riding safe and comfortable. In today's socio-economic situations, as pavement infrastructures have aged, road agencies need to constantly monitor pavements to locate unacceptable and severe surface irregularities for the welfare of road users.

Although maintenance criteria for overall surface smoothness are satisfied, the localized surface irregularities due to road structures, distresses, etc., have reduced the ideal qualities of pavements. In cold regions including Hokkaido, Japan, frost heaving particularly causes a major factor of localized distress that yields surface cracks and bumps. A technique for detecting localized irregularities activities is highly required for daily pavement monitoring.

A distress survey commonly uses visual-based methods. Conventional techniques subjectively survey the distress by visual inspections, which can be implemented simply and inexpensively, but are not objective and require too much time. More current approaches objectively record the distress by use of automated detection equipment based on video/ photographic images, which are generally more expensive to carry out than the subjective method. Thus, the objective techniques are only used once in three years by expressway agencies in Japan due to the initial and running costs of the equipment.

Since modern technologies improve road surface condition survey with better sensors, many response-type profilers to estimate the International Roughness Index (IRI) as the standard scale of predicting roughness conditions have been introduced[1),2)]. As response-type profilers are intended to measure the IRI, the question arises as to how the users of the profilers could identify the location and type of surface distress in measured profile data.

The objective of this study is to develop a method for detecting the location and type of severe surface distress due to frost heaving measured by use of a response-type mobile profilometer (MPM). Although the MPM uses accelerometers, it can measure the surface profile. This function helps to extract the information about distress characteristics of the

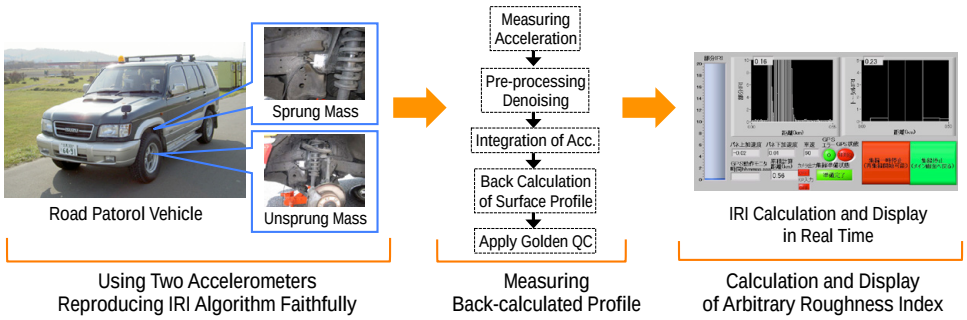

Fig. 1 Measurement Principle of the Response-type Profiler.

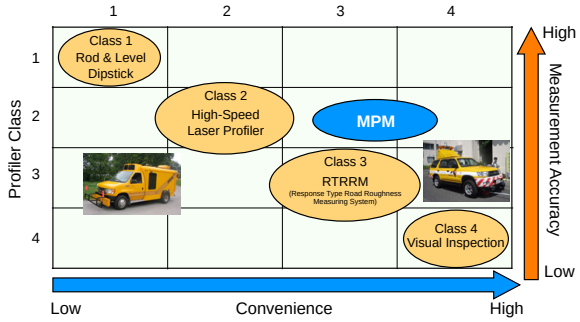

Fig. 2 Classification of Profilers.

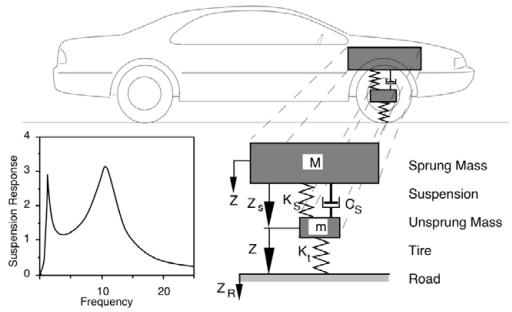

Fig. 3 QC Model[7].

profiles.

A technique conventionally applied to extract the information of interest in roughness profile data is the signal processing called “filtering”. Unlike the conventional convolution- and Fourier-based filtering techniques, the wavelet transform (WT) operates as directional filters that treat downward waveforms differently from upward ones. The WT has found various applications in engineering fields including surface profile analyses[3),4)].

A major remaining problem in the use of the WT has been the selection of a basic function suitable for profile analyses. Since second generation wavelets based on the lifting scheme theory were proposed [5)], this problem has been solved. A concept of the lifting scheme concentrates on the improvement of an existing WT by adding controllable free parameters to original basic functions[6)]. This technique enables us to develop customized lifting wavelet filters extracting desirable waveform characteristics. In this study, we construct the lifting wavelet filters to detect the surface distress due to frost heaving.

2. ROAD SURFACE MONITORING BY USE OF THE MPM

(1) Overview of the MPM

The MPM consists of two small accelerometers, which can be simply attached to a suspension system for any passenger and commercial vehicles. The principle of this profilometer is faithful to the standard quarter-car (QC) model used for the IRI calculation. **Fig. 1** shows the measurement principle of the MPM. As shown in the figure, a surface profile can be measured by back calculation analyses after the pre-processing that removes the noise, direct current excitation, and velocity dependence factors of vehicle vibrations. Then, the standard QC model is applied to the measured profile data to calculate the IRI. **Fig. 2** shows the profiler classification and the target of the MPM. The measurement algorithm of the MPM combines the accuracy of Class 2 measures and the convenience of Class 3 measures[2)].

(2) QC model

The QC model is a mathematical model of a vehicle that represents a body and a single wheel as shown in **Fig. 3**[7)]. The QC model predicts the spatial derivative of suspension stroke in response to a profile using standard settings called Golden Car Parameters for speed and the vehicle properties[8)]. The IRI can be calculated by use of the QC model applied to a measured longitudinal surface profile.

(3) Roughness profile calculation

The mathematical procedure in calculating IRI can be described as a filtering algorithm using QC filter of which response is shown in **Fig. 4**. The QC filter weighs the wavelengths of a slope profile between 0.1 and 100m to gain the roughness characteristics. The filtered profile is generally called roughness profile. The IRI is an accumulation of absolute values of a roughness profile normalized by a certain driving distance. Thus, a roughness profile clearly reflects the functional perspectives of surface characteristics such as ride quality and driving safety. The automatic distress detection executed

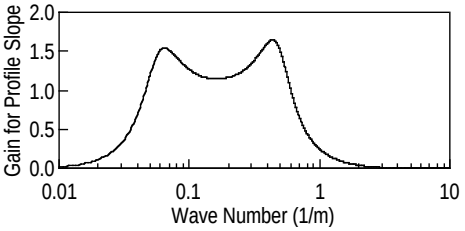

Fig. 4 Response of the QC Model.

by using a roughness profile contributes to the planning of maintenance and rehabilitation projects for improving the serviceability to road users. This study discusses a potential application of the MPM to detect the surface distress due to frost heaving in the roughness profile measurements.

3. LIFTING SCHEME THEORY FOR DISTRESS DETECTION

Convolution- and Fourier-based filters that are generally used for profile analyses may detect wanted/unwanted geometrical characteristics included in a roughness profile. However, these filters are non-directional filters that consider positive (e.g., bumps) and negative (e.g., cracks) waveforms in a target wavelength as the same sinusoids and thus cannot distinguish between upward and downward surface faults. Against the conventional methods, the WT executes directional filtering using lifting scheme.

(1) Overview of wavelet transform (WT)

In a general WT, a roughness profile is analyzed at different frequency bands with different resolution by decomposing the profile into components consisting of a coarse approximation (low-frequency component) supplemented by detailed information (high-frequency component). The approximation can be then further decomposed to provide more detailed information. This means that the WT, especially for discrete transform, can perform multiresolution analysis using a fast pyramid algorithm.

(2) Lifting scheme

A wide selection of basic function forms of the WT is available for different applications based on the characteristics of the signal concerned. However, the selection of a basic function is a problem of the WT. The second generation wavelets based on the lifting scheme, on the other hand, enhance the WT by making lifting wavelet filters[9]. A lifting wavelet filter set contains controllable free parameters constructed from initial biorthogonal wavelet filter set. Free parameters can be learned from training signals that include wave form characteristics of a target distress for the detection. The following section describes the mathematical descriptions of automatic distress detection based on the lifting scheme.

(3) Automatic distress detection method based on the lifting scheme

a) Theory of wavelet transform[5),6),9)]

Let c_l^1 denote a roughness profile with distance parameter l. Using multiresolution analysis in the WT, the roughness profile can be decomposed into low-frequency and high-frequency components as follows:

$$\hat{c}_m^0 = \sum_l \tilde{\lambda}_{l-2m} c_l^1 \tag{1}$$

$$\hat{d}_m^0 = \sum_l \tilde{\mu}_{l-2m} c_l^1 \tag{2}$$

where $\tilde{\lambda}_m$ and $\tilde{\mu}_m$ are called decomposition filters. Conversely, the original roughness profile c_l^1 can be reconstructed from low-frequency and high-frequency components $\hat{c}_m^0$ and $\hat{d}_m^0$ by the formula:

$$c_l^1 = \sum_m \lambda_{l-2m} \hat{c}_m^0 + \sum_m \mu_{l-2m} \hat{d}_m^0 \tag{3}$$

where λ_m and μ_m are called reconstruction filters. For later convenience, the decomposition and reconstruction filters are denoted as

$$\begin{aligned} h_{k,l}^{old} &= \lambda_{k-2l}, \; g_{m,l}^{old} = \mu_{l-2m} \\ \tilde{h}_{k,l}^{old} &= \tilde{\lambda}_{k-2l}, \; \tilde{g}_{m,l}^{old} = \tilde{\mu}_{l-2m} \end{aligned} \tag{4}$$

The tuple of these filters $\{h_{k,l}^{old}, \tilde{h}_{k,l}^{old}, g_{k,l}^{old}, \tilde{g}_{k,l}^{old}\}$ satisfies the following biorthogonal conditions:

$$\begin{aligned} &\sum_l h_{k,l}^{old} \tilde{h}_{k',l}^{old} = \delta_{kk'}, \; \sum_l g_{m,l}^{old} \tilde{h}_{k,l}^{old} = 0 \\ &\sum_l h_{k,l}^{old} \tilde{g}_{m,l}^{old} = 0, \; \sum_l g_{m,l}^{old} \tilde{g}_{m',l}^{old} = \delta_{mm'} \end{aligned} \tag{5}$$

where δ indicates Kronecker delta. Note that l represents the frequency resolution parameter and k and m give the parameters of location for low- and high-frequency components.

b) Construction of lifting wavelet filters[5),6),9)]

Let $\{h_{k,l}^{old}, \tilde{h}_{k,l}^{old}, g_{k,l}^{old}, \tilde{g}_{k,l}^{old}\}$ denote a set of initial biorthogonal wavelet filters. A new set of biorthogonal wavelet filters $\{h_{k,l}, \tilde{h}_{k,l}, g_{k,l}, \tilde{g}_{k,l}\}$ is defined as follows:

$$\begin{aligned} h_{k,l} &= h_{k,l}^{old} + \sum_m \tilde{s}_{k,m} g_{m,l}^{old} \\ \tilde{h}_{k,l} &= \tilde{h}_{k,l}^{old} \\ g_{m,l} &= g_{m,l}^{old} \\ \tilde{g}_{m,l} &= \tilde{g}_{m,l}^{old} - \sum_k \tilde{s}_{k,m} \tilde{h}_{k,l}^{old} \end{aligned} \tag{6}$$

where $\tilde{s}_{k,m}$ denote free parameters, $\tilde{h}_{k,l}$ and $\tilde{g}_{m,l}$ indicate low- and high-pass decomposition filters, and $h_{k,l}$ and $g_{m,l}$ indicate low- and high-pass reconstruction filters. This algorithm can create a new filter set suitable for the automatic distress detection by adjusting free parameters. The biorthogonal conditions of a new filter set are as follows:

$$\sum_l h_{k,l}\tilde{h}_{k',l} = \delta_{kk'},\ \sum_l g_{m,l}\tilde{h}_{k,l} = 0$$
$$\sum_l h_{k,l}\tilde{g}_{m,l} = 0,\ \sum_l g_{m,l}\tilde{g}_{m',l} = \delta_{mm'} \quad (7)$$

c) Learning of free parameters [9)]

As shown in Equation (6), high-pass filters rather than low-pass filters are lifted in the decomposition process. Where an input roughness profile is again denoted as c_l^1, new high-frequency components by applying the new high-pass decomposition filters can be written as

$$d_m^0 = \sum_l \tilde{g}_{m,l} c_l^1 \quad (8)$$

This can be substituted based on Equation (6) as follows:

$$d_m^0 = \sum_l (\tilde{g}_{m,l}^{old} - \sum_k \tilde{s}_{k,m}\tilde{h}_{k,l}^{old}) c_l^1 = r_m - \sum_k a_k \tilde{s}_{k,m} \quad (9)$$

where r_m and a_k indicate the high- and the low-frequency components resulted from the decomposition using the old filters, that is,

$$r_m = \sum_l \tilde{g}_{m,l}^{old} c_l^1,\ a_k = \sum_l \tilde{h}_{k,l}^{old} c_l^1 \quad (10)$$

Free parameters $\tilde{s}_{k,m}$ can be determined so as to vanish the high-frequency component d_m^0 in Equation (9). In other words, surface distress in the roughness profile can be detected by putting

$$d_m^0 = r_m - \sum_k a_k \tilde{s}_{k,m} = 0 \quad (11)$$

To learn the free parameters $\tilde{s}_{k,m}$, the algorithm requires $2n$ training signals $c_l^{1,\nu}$ ($\nu = 1,2,\ldots,2n$) that include desired profile features. The training signals define the type and severity of the surface distress that should be detected. Then, the following condition is imposed:

$$\sum_{k=m-n}^{m+n} a_k^{\nu} \tilde{s}_{k,m} - r_m = 0, \quad \nu = 1,2,\ldots 2n \quad (12)$$

where

$$r_m^{\nu} = \sum_l \tilde{g}_{m,l}^{old} c_l^{1,\nu},\ a_m^{\nu} = \sum_l \tilde{h}_{k,l}^{old} c_l^{1,\nu} \quad (13)$$

Although the number of equations in Equation (12) is $2n$, unknown variables $\tilde{s}_{k,m}$ are $2n+1$. However, the following equation is consequentially identified because the summation of the high-pass filters $\tilde{g}_{m,l}$ must be zero, that is,

$$\sum_l \tilde{g}_{m,l} = \sum_l (\tilde{g}_{m,l}^{old} - \sum_{k=m-n}^{m+n} \tilde{s}_{k,m}\tilde{h}_{k,l}^{old}) = 0 \quad (14)$$

Since $\tilde{g}_{m,l}^{old}$ satisfy $\sum_l \tilde{g}_{m,l}^{old} = 0$, this condition is equivalent to

$$\sum_{k=m-n}^{m+n} \tilde{s}_{k,m} = 0 \quad (15)$$

Summarizing Equation (12) and (15) in the matrix form results in the following equation:

$$\begin{bmatrix} a_{m-n}^1 & a_{m-n+1}^1 & \cdot & a_{m+n}^1 \\ a_{m-n}^2 & a_{m-n+1}^2 & \cdot & a_{m+n}^2 \\ \cdot & \cdot & \cdot & \cdot \\ \cdot & \cdot & \cdot & \cdot \\ a_{m-n}^{2n} & a_{m-n+1}^{2n} & \cdot & a_{m+n}^{2n} \\ 1 & 1 & \cdot & 1 \end{bmatrix} \begin{bmatrix} \tilde{s}_{m-n,m} \\ \tilde{s}_{m-n+1,m} \\ \cdot \\ \cdot \\ \tilde{s}_{m+n-1,m} \\ \tilde{s}_{m+n,m} \end{bmatrix} = \begin{bmatrix} r_m^1 \\ r_m^2 \\ \cdot \\ \cdot \\ r_m^{2n} \\ 0 \end{bmatrix} \quad (16)$$

This equation can be solved by the Gaussian elimination. Substituting the solutions $\tilde{s}_{k,m}$ into Equation (6), lifting wavelet filters can be produced.

d) Automatic distress detection method [9)]

Once lifting wavelet filters are constructed, the locations of surface distress in the roughness profile that is similar to the training signals can be automatically detected. The high-frequency components $\hat{d}_m^0$ and d_m^0 are calculated by the old and lifting high-pass wavelet filters $\tilde{g}_{m,l}^{old}$ and $\tilde{g}_{m,l}$ from c_l^1 by use of Equation (2) and (8). Here, remember that the free parameters $\tilde{s}_{k,m}$ of the lifting wavelet filters $\tilde{g}_{m,l}$ are optimized to vanish d_m^0 at the locations of target distresses. A possible strategy is to find the location m that makes $d_m^0 = 0$. Unfortunately, this strategy may detect the location m other than the target points that their high-frequency components are almost zero for both $\hat{d}_m^0$ and d_m^0. To avoid this kind of false detections, a method that searches c_l^1 to find the location m so as to maximize the quantity

$$I_m = \left|\hat{d}_m^0\right| - \left|d_m^0\right| \quad (17)$$

is suggested. When the value $I_m > 0$ is larger than a certain threshold value, the location m is regarded as the learned surface distress; and thus, can become a detection index.

4. AUTOMATIC DISTRESS DETECTION USING THE MPM

In this study, performance of lifting scheme for automatic distress detection using the MPM is examined by comparing with a result of rod and level survey. The validation experiment was performed on a frost-heaved expressway in March 2013 in service in Hokkaido, Japan.

(1) Surface monitoring data

For the purpose of the validation experiment, surface distresses were manually recorded by photographic images. Reference true profile was also manually measured by the rod and level as a Class 1 measure. **Fig. 5** shows the overview of experimental site and the condition of rod and level survey. The surface profiles were simultaneously measured by use of the MPM equipped for a passenger vehicle with three different speeds of 60, 80, and 100km/h. Then, the QC simulation computed a roughness pro-

(a) Experimental Site **(b)** Rod and Level Survey

Fig. 5 Overview of the Experimental Site and the Condition of Rod and Level Survey.

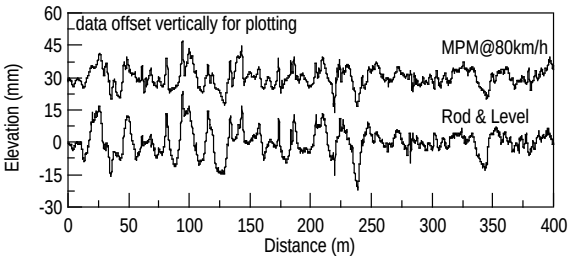

(a) Surface Profiles

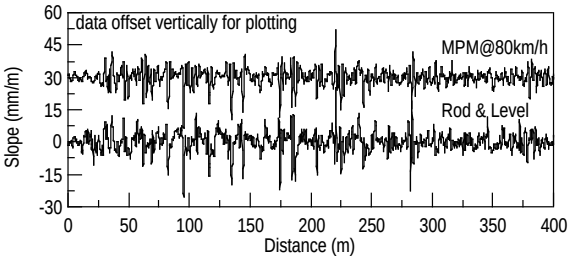

(b) Roughness Profiles

Fig. 6 Examples of Surface Monitoring Data.

(a) *l*=184.0m **(b)** *l*=204.0m

Fig. 7 Example Images of Surface Distress due to Frost Heaving.

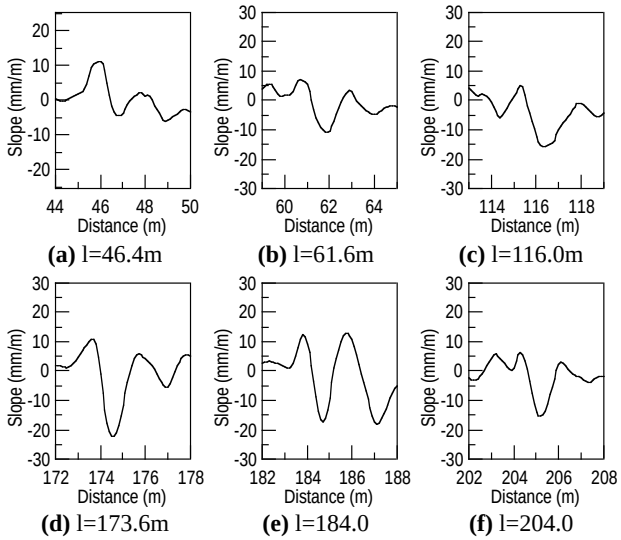

(a) l=46.4m **(b)** l=61.6m **(c)** l=116.0m

(d) l=173.6m **(e)** l=184.0 **(f)** l=204.0

Fig. 8 Training Signals of the Roughness Profile Measured by the Rod and Level.

file for each profiler. The experimental section was 400m long, and the measured profiles were sampled at an interval of 100mm for the present study. The measured surface and roughness profile data are shown in **Fig. 6**. The profiles measured by the MPM are recorded at the driving speed of 80km/h in the figure. As shown in the figure, both profiles are fairly corresponded closely (the average cross correlation-coefficient = 0.80).

(2) Construction of lifting wavelet filters

a) Training signals

According to the manual distress survey, the experimental section has a number of severe surface distresses due to frost heaving. The distresses appeared irregularly and consisted of high severity transverse cracks around heaved pavement surfaces as shown in **Fig. 7**. They consequently reduce the ride quality of traveled vehicles. Thus, this type of distress is an important aspect of pavement management especially for cold regions. This study defines the distress due to frost heaving as the target for training signals, which is a good example for the experimental validation of the automatic distress detection.

In the experimental section, we had twenty-four distresses in the pavement surface. Too much longer training signals generally lead to missdetection because a roughness profile is averaged more than necessary. In the present research, six high severity distresses are prepared as training signals $c_l^{1,v}$ ($v = 6$). **Fig. 8** shows training signals that are measured by the rod and level. Here, the locations *l*=95.2m and *l*=220m were excluded from the analysis because they were due to the surface patch and pavement joint.

b) A set of initial wavelet filters

A wide selection of basic function forms of the WT is available for different applications based on the characteristics of the signal concerned. In this study, the biorthogonal reconstruction and decomposition filters with 2 and 4 vanishing moments were selected as a set of initial wavelet filters. This filter set consists of comparatively short digital filters, and is associated with the basic function that has a sharp peak. Although lifting wavelet filters can be constructed from arbitrary filter sets, the features of the initial wavelet filters are advantageous to deal with surface distress data. **Table 1** describes the set of initial wavelet filters $\{h_{k,l}^{old}, \tilde{h}_{k,l}^{old}, g_{k,l}^{old}, \tilde{g}_{k,l}^{old}\}$.

c) Learning free parameters and filter design

As a pre-processing, a multiresolution analysis based on the conventional WT examined the dominant waveband of the target distress. According to the analysis, the target distress occurs in the decom-

Table 1 Initial Wavelet Filters.

k, m	$h_{k,l}^{old}$	$\tilde{h}_{k,l}^{old}$	$g_{m,l}^{old}$	$\tilde{g}_{m,l}^{old}$
0	0.7071	0.9944	-0.9944	-0.7071
1, -1	0.3536	0.4198	0.4198	0.3536
2, -2	-	-0.1768	0.1768	-
3, -3	-	-0.0663	-0.0663	-
4, -4	-	0.0331	-0.0331	-

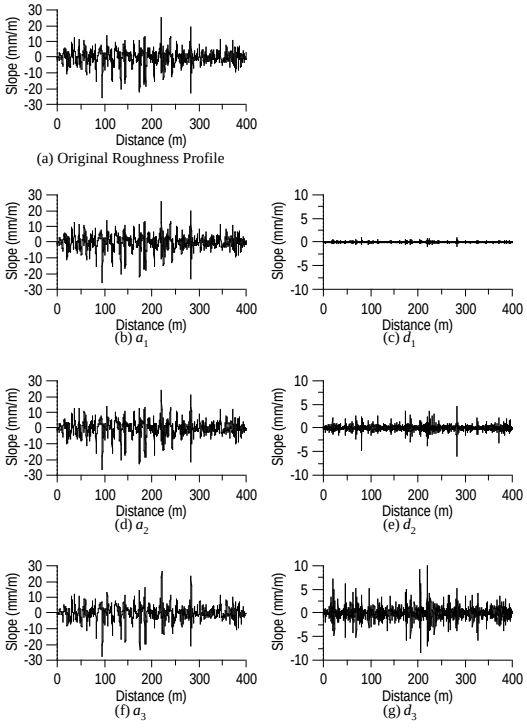

Fig. 9 A Multiresolution Analysis using Initial Wavelet Filters (Rod and Level).

position level 3, as shown in **Fig. 9**, of which high-frequency components correspond to the wavelengths of 0.8 to 1.6m. Thus, free parameters are learned from Level 3 components of the multiresolution analysis using the initial wavelet filters. As the $c_l^{1,\nu}$ ($\nu = 1,2,3,4,5,6$) denote the training signals as shown in **Fig. 8**, the free parameters for each roughness profile measurement can be determined by using Equation (16) as shown in **Table 2**. Using these parameters, lifting wavelet filters $\{h_{k,l}, \tilde{h}_{k,l}, g_{k,l}, \tilde{g}_{k,l}\}$ have been created based on Equation (6). **Table 3** and **Table 4** summarize lifted high-pass decomposition filters and low-pass reconstruction filters, respectively.

(3) Automatic distress detection result

After the calculation of $\hat{d}_m^0$ and d_m^0, the quantified index I_m identifies the location of target distresses. Here, I_m can be easily calculated by substituting Equation (9) for Equation (17) as follows:

$$I_m = \left|\hat{d}_m^0\right| - \left|r_m - \sum_k a_k \tilde{s}_{k,m}\right| \qquad (18)$$

Fig. 10 shows the result of automatic distress detection using Equation (18). In the figure, the arrows designate the locations of the target distresses and the I_m values are normalized so that the maximum I_m for the training location can be $I_{m,\max} = 1$. The locations that are $I_m > 0$ potentially correspond to the target distress learned as the training signals. For the purpose of pavement monitoring activities, we suggest the following two possible ideas to decide a threshold of the quantified index I_m.

a) $I_m > 0$: This means that all the locations that are $I_m > 0$ are considered as the distress from a fail-safe perspective.

b) $I_m \geq I_{m,\min}$: This means that the minimum I_m value at the trained location is set as a threshold to monitor distressed points severely.

As accuracy evaluation of the automatic distress detection results, we evaluated the percentage of the following items:

- correct detection: locations of the distress can be successfully detected,
- incorrect detection: non-distressed locations are detected in error.

In case of a) $I_m > 0$, the following is also calculated:

- miss detection: locations of the distress are missed in the process.

Table 5 summarizes the accuracy evaluation results. As shown in the table, the severe monitoring using the criterion of $I_m \geq I_{m,\min}$ clearly emphasizes

Table 2 Free Parameters.

k	Rod and Level	MPM @60km/h	MPM @80km/h	MPM @100km/h
m-3	-0.6858	0.4671	0.0570	-0.3670
m-2	0.3132	-0.3202	-0.6760	-0.1640
m-1	0.2587	0.2960	0.1036	0.2097
m	-0.3072	-0.2518	0.2468	-0.1451
m+1	-0.0312	-0.1064	-0.0932	-0.2055
m+2	0.4029	0.0749	0.2419	0.5281
m+3	0.0494	-0.1595	0.1199	0.1438

Table 3 Lifted High-pass Decomposition Filters.

k, m	Rod and Level	MPM @60km/h	MPM @80km/h	MPM @100km/h
-4	0.0377	0.0700	0.1717	0.2604
-3	-0.1731	-0.0140	-0.0381	-0.1355
-2	-0.0337	0.2404	0.1096	-0.1776
-1	-0.8990	-0.6786	-0.8652	-1.0028
0	0.3767	0.5290	0.2802	0.3108
1	0.0060	0.0719	-0.0343	-0.0254
2	-0.0046	-0.0307	0.0132	0.0079
3	0.0033	-0.0106	0.0079	0.0095
4	-0.0016	0.0053	-0.0040	-0.0048

Table 4 Lifted Low-pass Reconstruction Filters.

k, m	Rod and Level	MPM @60km/h	MPM @80km/h	MPM @100km/h
-4	0.0377	0.0700	0.1717	0.2604
-3	0.1731	0.0140	0.0381	0.1355
-2	-0.0337	0.2404	0.1096	-0.1776
-1	0.8990	0.6786	0.8652	1.0028
0	0.3767	0.5290	0.2802	0.3108
1	-0.0060	-0.0719	0.0343	0.0254
2	-0.0046	-0.0307	0.0132	0.0079
3	-0.0033	0.0106	-0.0079	-0.0095
4	-0.0016	0.0053	-0.0040	-0.0048

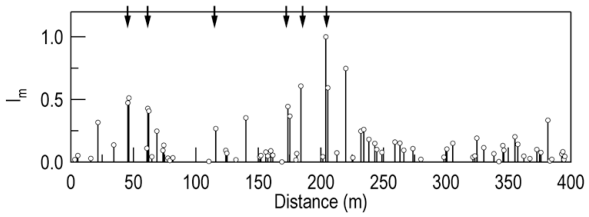

(a) Rod and Level

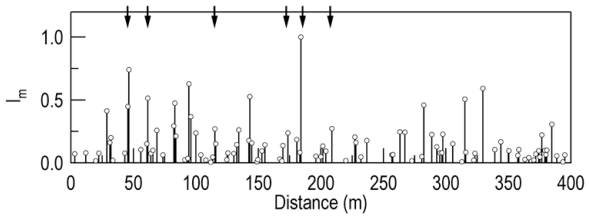

(b) MPM at 60km/h

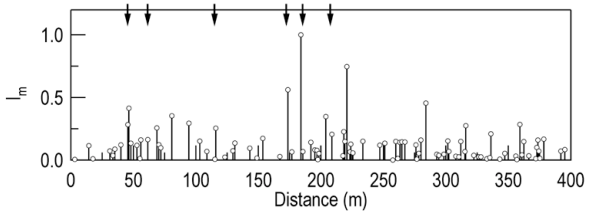

(c) MPM at 80km/h

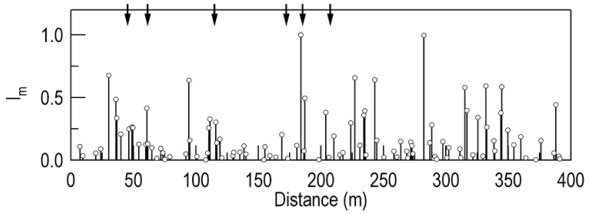

(d) MPM at 100km/h

Fig. 10 Automatic Distress Detection Results.

the location of target distress, considering that the mean percentage of correct detection is 77.8% (incorrect of 22.2%). On the other hand, the mean percentages of the correct, incorrect, and missdetection are 62.5%, 35.0%, and 2.5%, respectively for $I_m > 0$. Here, note that the acceptable error for longitudinal profile measurements in Japan is within 30%. Thus, the performance of the proposed method satisfies the practical requirements of pavement monitoring and distress survey. These results indicate that the lifting scheme enables us to monitor severe surface distresses due to frost heaving by use of the MPM without visual-based methods.

Although this paper describes a particular distress case, the results demonstrate the significant findings of which the lifting scheme is available for the automatic distress detection by use of a MPM. A threshold value will be improved by further researches that depend on an employed profiler and its operation. This study contributes to the implementation of more effective daily road patrol.

5. CONCLUSIONS

In recent years, road agencies initiate the development of a quantitative, efficient, and economical pavement monitoring method for the daily inspection of their pavements. This paper introduced a mobile profilometer (MPM) by use of accelerometers to regular monitoring of expressways. In this study, we examined the potential application of the MPM to automatic distress detection based on the lifting scheme theory. The lifting scheme constructs custom wavelet filters that contain controllable free parameters, and then performs decomposition and reconstruction by use of the filters.

Table 5 Accuracy of Automatic Distress Detection.

	Rod and Level		MPM@60km/h	
	$I_m > 0$	$I_m \geq I_{m,\min}$	$I_m > 0$	$I_m \geq I_{m,\min}$
Correct (%)	62.5	77.8	60.0	83.3
Incorrect (%)	32.5	22.2	37.5	16.7
Miss (%)	5.0	-	2.5	-
	MPM@80km/h		MPM@100km/h	
	$I_m > 0$	$I_m \geq I_{m,\min}$	$I_m > 0$	$I_m \geq I_{m,\min}$
Correct (%)	67.5	73.3	60.0	76.9
Incorrect (%)	32.5	26.7	37.5	23.1
Miss (%)	0.0	-	2.5	-

The lifting scheme identifies the locations of surface distress by seeking a distance *m* of being the quantitative index $I_m > 0$. For the purpose of pavement monitoring activities, we suggested two criteria for I_m , namely, $I_m > 0$ and $I_m \geq I_{m,\min}$. This paper illustrated the practical demonstration of identifying the distress due to frost heaving. According to the result, the severe monitoring using the criterion of $I_m \geq I_{m,\min}$ clearly emphasized the location of target distress, considering that the mean percentage of correct detection is 77.8% (incorrect of 22.2%). On the other hand, as for $I_m > 0$, the mean percentages of the correct, incorrect, and missdetection were 62.5%, 35.0%, and 2.5%, respectively. Considering the acceptable error for longitudinal profile measurements, the performance of the proposed method satisfies the practical requirements of pavement monitoring and distress survey.

This study contributes to the distress survey using MPMs rather than visual-based methods. Although this paper demonstrated a particular distress case, the lifting scheme that constructs different lifting wavelet filters can be applied various types of distress such as pothole, patching, etc. by learning different free parameters.

ACKNOWLEDGMENT: This work was supported by JSPS KAKENHI Grant Number 25870026.

REFERENCES

1) Katicha, S.W., Flintsch, G.W., and Fuentes, L.G.: Use of Probe Vehicle to Measure Road Ride Quality, *Proceedings of Transportation Research Board 93rd Annual Meeting*, Paper No. 14-2836, 2014.

2) Tomiyama, K., Kawamura, A., Nakajima, S., Ishida, T., and Jomoto, M.: A Mobile Data Collection System Using Accelerometers for Pavement Maintenance and Rehabilitation, *Proceedings of 8th International Conference on Managing Pavement Assets*, Paper No. 142 (CD-ROM), 2011.
3) Yi, P., Sheng, L., and Yu, L.: Wavelet Transform For Feature Extraction to Improve Volume Adjustment Factors for Rural Roads, Transportation Research Record, No. 1879,pp. 24-29, 2004.
4) Shokouhi, P., Gucunski, N., Maher, A., and Zaghloul, S.M.: Wavelet-Based Multiresolution Analysis of Pavement Profiles as a Diagnostic Tool, Transportation Research Record, No. 1940, pp.79-88, 2005.
5) Sweldens, W: The Lifting Scheme: A Construction of Second Generation Wavelets, *SIAM Journal on Mathematical Analysis*, Vol. 29, No. 2, pp. 511-546, 1997.
6) Jansen, M., and Oonincx, P.: Second Generation Wavelets and Application, Springer, 2004.
7) Gillespie, T.D.: Everything You Always Wanted to Know about the IRI, But Were Afraid to Ask!, Presented at the Road Profile Users Group Meeting, Nebraska, 1992.
8) Sayers, M. W. and Karamihas, S. M.: The Little Book of Profiling, - Basic Information about Measuring and Interpreting Road Profiles, The University of Michigan, 1998.
9) Takano, T., Minamoto, H., Arimura, K., Niijima, T., Iyemori, T., and Araki, T.: Automatic detection of geomagnetic sudden commencement using lifting wavelet filters, *Proceedings of the Second International Conference on Discovery Science*, pp. 242-251, 1999.

(Received May 14, 2014)